Mechanistic Guidance Leads to Enhanced Site-Selectivity in C–H Oxidation Reactions Catalyzed by Ruthenium bis(Bipyridine) Complexes

Jeremy D. Griffin[†], David B. Vogt[†], Justin Du Bois[*,‡], and Matthew S. Sigman[*,†]

[†] Department of Chemistry, University of Utah, 315 South 1400 East, Salt Lake City, Utah 84112, United States.
[‡] Department of Chemistry, Stanford University, 337 Campus Drive, Stanford, CA 94305, United States.

Supporting Information Placeholder

ABSTRACT: The development of an operationally simple C–H oxidation protocol using an acid-stable, bis(bipyridine)Ru catalyst is described. Electronic differences remote to the site of C–H functionalization are found to affect product selectivity. Site selectivity is further influenced by the choice of reaction solvent, with highest levels of 2° methylene oxidation favored in aqueous dichloroacetic acid. A statistical model is detailed that correlates product selectivity outcomes with computational parameters describing the relative 'electron-richness' of C–H bonds

Keywords: C–H oxidation, ruthenium, catalysis, regioselective, organic reactions, Brønsted acid

One of the central challenges of modern organic chemistry is the selective functionalization of inert C–H bonds. Selective oxidation of sp^3 C–H bonds has historically been accomplished using stoichiometric reagents such as dioxiranes,[1–9] hypervalent iodine reagents (IBX, etc.),[10–14] or catalytic chromium-based oxidants.[15,16] These reagents are generally selective for the oxidation of tertiary (3˚) or benzylic sites, whereas relatively unactivated secondary (2˚) and primary (1˚) C–H bonds are typically unreactive. Methyl(trifluoromethyl)dioxirane (TFDO) has been demonstrated to oxidize unactivated 2˚ C–H bonds;[5] however, reactions with TFDO require low temperatures and extended reaction times to achieve respectable levels of site-selectivity (**Figure 1**). More recent advancements have enabled site-selective functionalization of 2˚ sites with distal deactivating groups. Utilization of first row transition metal complexes derived from Fe[17–25] or Mn[26–30], which generate electrophilic metal-oxo intermediates, have enabled discrimination between electronically differentiated 2˚ C–H bonds. A recent resurgence of interest in electrochemical oxidation has demonstrated the power of this technology for functionalizing aliphatic C–H bonds.[31,32] Since the effective redox mediators (quinuclidine) operate through electron deficient radicals, these methods are similarly selective for 'electron-rich' C–H bonds, giving comparable reaction outcomes to metal-oxo based technologies (**Figure 1**).

Our labs have reported that bis(bipyridine)Ru complexes catalyze the selective oxidation of 3˚ C–H bonds distal to ammonium salts with high positional selectivity.[33,34] Analogous to other C–H oxidation methods, which proceed through high-valent metal-oxo intermediates, selective oxidation of distal 2˚ C–H bonds was shown to be achievable (a single example was demonstrated) in substrates absent 3˚ or benzylic C–H bonds. Literature precedent[35] as well as our own mechanistic studies of this process revealed that oxidation likely proceeds by way of Ru(V) or Ru(IV) oxo– or dioxo– intermediates.[36] Several potential mechanisms for catalyst deactivation were also identified, including oxidation of the dissociated bipyridine ligand to yield the corresponding bipyridine *N*-oxide and dimerization of interme-

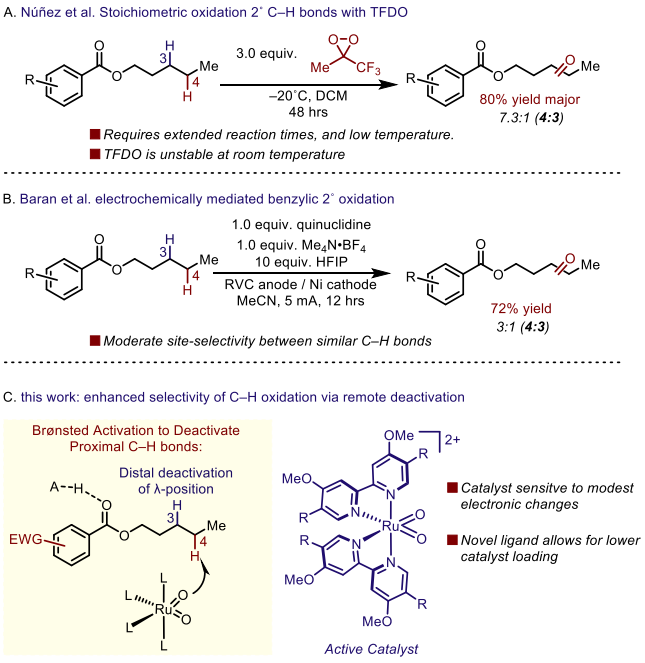

Figure 1: (**A**) Stoichiometric TFDO for selective remote 2˚ C–H oxidation (**B**) Modern approach to undirected C–H oxidation (**C**) Augmenting the inherent site-selectivity of Ru catalyzed C–H oxidation catalysts.

diate Ru species. These decomposition pathways are responsible for low catalyst turnover numbers (TONs), a problem that

plagues many other C–H oxidation methods and is likely a consequence of the highly reactive intermediate species necessary to achieve undirected C–H functionalization. The identity of the ligand(s) therefore has a significant impact on catalyst lifetime and turnover numbers (TONs).

Another common limitation in these methods is that site-selectivity of oxidation predominantly relies on the intrinsic differences in reactivity of C–H bonds within a given substrate. Thus, two hypotheses were formulated with the goal of improving reaction performance in terms of both site-selectivity and reactivity: 1) higher selectivity could be achieved by judicious selection of remote functional groups, which are designed to deactivate the proximal C–H bonds. 2) TONs could be enhanced using catalysts bearing electron-rich bipyridine ligands, thereby limiting undesired ligand loss from the high-valent Ru species. Herein, we describe the successful implementation of these ideas, which have resulted in the development of a Ru complex capable of achieving selective 2˚ C–H bond oxidation with generally higher TONs.

Table 1: Probing Changes to Remote Electronic Effects.[a]

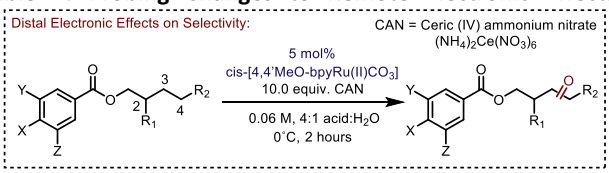

A

entry	substituent	acid	combined yield[b] (SM)[c]	(4:3)[d]
1	X = H	AcOH	64% (21%)	2.8:1
2	X = CF_3	AcOH	80% (14%)	3.5:1
3	X = CN	AcOH	82% (17%)	4.4:1
4	X = NO_2	AcOH	79% (11%)	4.3:1
5	X = H	DCAA	63% (11%)	4.7:1
6	X = NO_2	DCAA	77% (21%)	8.0:1
7	X = NO_2 at –10˚C	DCAA	45% (56%)	~10:1
8	Y = NO_2 Z = NO_2	DCAA	88% (0%)	9.2:1

B

entry	substituent	acid	combined yield[b] (SM)[c]	(3:2)[d]
9	X = H	AcOH	80% (11%)	0.7:1
10	X = NO_2	AcOH	81% (17%)	0.9:1
11	X = H	DCAA	65% (6%)	0.9:1
12	X = NO_2 6 hrs	DCAA	72% (21%)	1.8:1

Selectivity for oxidation reversed based on proximity to EWG

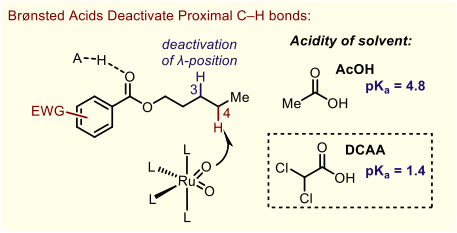

[a] 0.1 mmol scale. [b]Yield determined by ^{1}H NMR integration against HMDSO internal standard. [c]Yield of remaining starting material. [d]Ratio of the major and minor isomers.

In revisiting our earlier work with insights garnered through our mechanistic studies, we found *cis*-[4,4'-MeO-bpyRu(II)CO_3] as a pre-catalyst in combination with cerium (IV) ammonium nitrate (CAN) as a stoichiometric chemical oxidant to be effective for functionalization of the distal 2˚ C–H bond in substrate **A** (**Table 1**). However, as is observed with other C–H oxidation methods, only a modest selectivity of 2.8:1 was obtained between the C3 and C4 positions of pentylbenzoate (**entry 1**). To further probe how distal electronic effects influence regioselectivity, the identity of the remote functional group was varied wherein a more electron-withdrawing protecting group was found to improve selectivity for the C4 product (**Table 1 entries 2-4)**. Notably, selectivity for the 4-position was improved from 2.8:1 to 4.3:1 in switching from the benzoate (Bz) to 4–nitrobenzoate (4–NBz) group. Considering that bis(bipyridine)Ru complexes are stable under highly acidic conditions, we hypothesized that a Brønsted acid could be used to further deactivate C–H bonds in close proximity to Lewis basic electron-withdrawing groups (EWGs). Ultimately, we discovered that changing from acetic acid to a more acidic solvent such as dichloroacetic acid (DCAA, pK_a = 1.4)[37], with water as a co-solvent, led to improvement in site-selectivity (**entry 5**). The more acidic trifluoroacetic acid (TFA) proved ineffective likely due to the insolubility of CAN under these conditions. Several other potential acidic solvents were found to be reactive with the Ru complex (e.g., formic acid) (See Supporting information for details). The cooperative effect of having an electron-withdrawing functional group in the presence of a strong Brønsted acid was found to markedly improve site-selectivity from ~3:1 to 8:1 (**entry 6**). Further deactivation of proximal C–H bonds was accomplished using 3,5-dinitrobenzoyl (DNBz) as a protecting group, improving site-selectivity to 9.2:1 (**entry 7**).

Our results with substrate **A** extend to other esters (**entries 9-12).** Typically, 3˚ C–H bonds are more prone to oxidation as evidenced by entry 9 in which 3˚ C–H oxidation (C2) is slightly favored regardless of the ester group. However, the combination of 4-nitrobenzoate and DCAA cosolvent led to a reversal of site selectivity (**entry 12**). The need for a longer reaction time (6 vs 2h) with this starting material is consistent with the strong deactivating effect that DCAA imparts on all C–H bonds in the substrate.

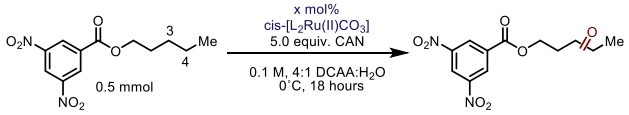

L1

catalyst loading	combined yield[a] (SM)[b]	(4:3)[c]
5 mol% :	76% (14%)	9.5:1
2.5 mol%:	59% (25%)	9.5:1
1 mol% :	29% (57%)	10:1

L2

catalyst loading	combined yield[a] (SM)[b]	(4:3)[c]
5 mol% :	74% (21%)	7.7:1
2.5 mol%:	73% (24%)	8.0:1
1 mol% :	48% (52%)	7.5:1

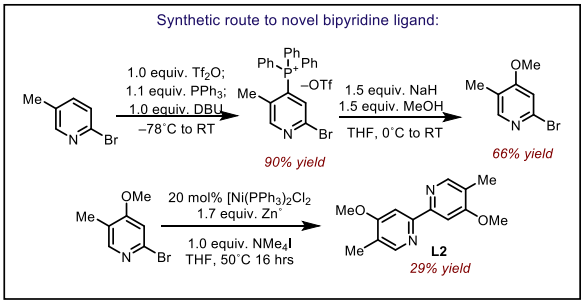

Figure 2: Comparison of **L1** and **L2**, and the synthetic route to **L2**. [a] Yield determined by ^{1}H NMR integration against HMDSO internal standard. [b]Yield of remaining starting material. [c]Ratio of the major and minor isomers.

As a final improvement to this method, we sought to identify a substituted bipyridine ligand that would enable lower catalyst loadings. Since high TONs are often difficult to attain for

highly reactive C–H oxidation catalysts, high loadings of catalyst are often utilized. We hypothesized that more electron rich bipyridine ligands would extend catalyst lifetimes, as stronger σ-donation would disfavor ligand dissociation from high-valent Ru intermediates where ligand loss is likely to occur.[36] Reports of multi-substituted bipyridines are sparse in the literature and thus synthesis of 4 and 5 substituted bipyridines remains challenging. Accordingly, we developed a new synthetic route to substituted bipyridine ligands, enabled by recent disclosures by McNally and coworkers (**Figure 2**).[38,39] This chemistry provided access to **L2** in only three steps from commercial materials. Using this new ligand, the bis(bipyridine)$_2$RuCO$_3$ loading could be reduced to 2.5 mol% **2** without significant loss of product yield, albeit with moderately reduced regioselectivity, when compared to 5 mol%

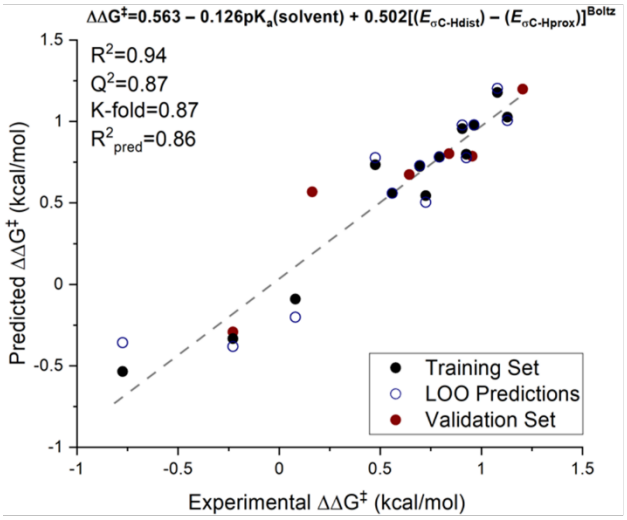

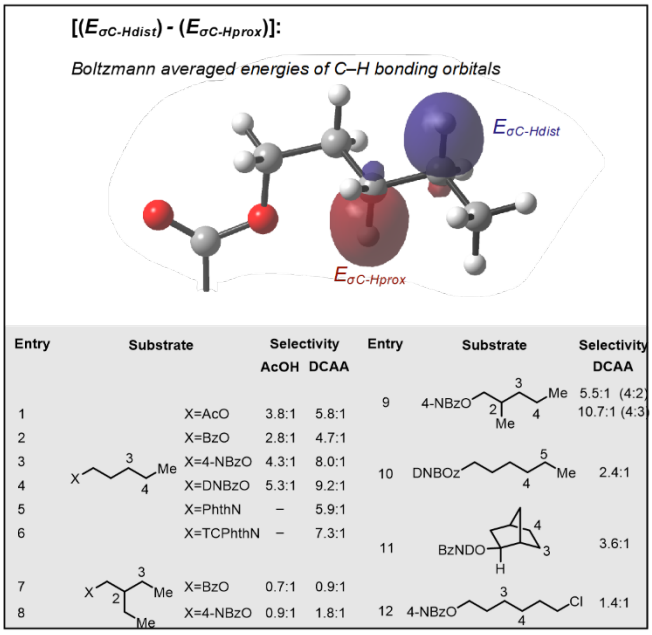

Entry	Substrate		Selectivity AcOH	Selectivity DCAA
1		X=AcO	3.8:1	5.8:1
2		X=BzO	2.8:1	4.7:1
3		X=4-NBzO	4.3:1	8.0:1
4		X=DNBzO	5.3:1	9.2:1
5		X=PhthN	–	5.9:1
6		X=TCPhthN	–	7.3:1
7		X=BzO	0.7:1	0.9:1
8		X=4-NBzO	0.9:1	1.8:1
9	4-NBzO		5.5:1 (4:2)	10.7:1 (4:3)
10	DNBOz		2.4:1	
11	BzNDO		3.6:1	
12	4-NBzO		1.4:1	

Figure 3: MLR model relating $(E_{\sigma C–Hdist} - E_{\sigma\ C–Hprox})^{Boltz}$ of various ester containing substrates, with the observed site-selectivity (expressed as ΔΔG‡). The pK_a of the acid solvent used in the reaction (AcOH or DCAA) functions as a binary classification parameter. Selectivity was obtained via analysis of crude ^{1}H NMR spectra.

RuL$_2$CO$_3$ using **L1**. While it is currently not clear how **L2** improves TONs, it is plausible that a slightly more electron rich bipyridine ligands could prevent loss of ligand in situ or promote oxidation to the higher Ru-oxidation states. Alternatively, it is feasible that the added steric bulk at the 5-position could disfavor formation of a crowded catalyst dimer.

To better understand the origin of selectivity in this Ru-catalyzed oxidation reaction, we pursued the development of statistical models that correlate site-selectivity to computationally (or experimentally) derived descriptors.[22] Developing a more robust understanding of how substrate and reaction conditions conspire to bias site selectivity could allow for more quantitative prediction of reaction outcomes.[40,41] While it has been suggested that electron-rich C–H bonds are often preferentially oxidized, it can be difficult to predict which C–H bonds qualify as such.[19,22] A modest set of primarily ester-containing substrates was synthesized to examine how different substrate structural changes impact selectivity (**Figure 3**). As these substrates have a somewhat large degree of conformational flexibility, conformational analysis of all of the substrates shown in Figure 2 was carried out using the OPLS3e forcefield in Macromodel,[42,43] using a 2.5 kcal/mol energy cutoff. The computed conformers were then optimized using DFT at the B3LYP/6-31+G(d,p) level of theory with single points taken at M06-2X/def2-TZVP.[44,45] Various substrate parameters were collected, and multivariate linear regression (MLR) analysis was performed using a forward stepwise linear regression algorithm.[41] A statistical model comprised of two terms was identified, which showed good correlation with the experimental data (R^2=0.94). A single term describing substrate electronic properties was necessary. The difference in energies of the σ-C–H bonding orbitals ($E_{\sigma C–H}^{Boltz}$) at the two competing sites of oxidation was found to have the strongest correlation with the observed site selectivity. Additionally, the other important parameter, pK_a of the co-solvent, was used as a binary classifier. Essentially, this parameter provides a means to unite the two data sets into a single predictive correlation. However, it does not necessarily allow for extrapolation to include other carboxylic acid solvents or conditions (See Supporting Information). It was found to be crucial to capture the conformational effects on relative C–H bond energy through Boltzmann averaging of the property from the representative set of conformers. Effectively, $E_{C–H}$ allows for quantification of the relative 'electron-richness' of a given C–H bond.

The utility of our statistical method was evaluated against a number of structurally disparate substrates. We elected to evaluate the majority of the substrate scope utilizing [4,4'-MeO-bpyRu(II)CO$_3$] as the ligand is accessed commercially**.** As depicted in Table 2, selective 2° C–H oxidation occurs in moderate to high yields. In most cases, the mass balance consisted of remaining starting material. Varying the identity of the electron-withdrawing group (EWG) has a profound effect on regioselectivity (**2a–2g**). The ratio observed in the formation of **2h** highlights that the difference in $E_{\sigma C–H}$ affected by EWGs is diminished

drastically by increased chain length when compared with **2a**. Reactions with substrates containing extended chains (**2i)** display improved 2˚:3˚ selectivity; highlighting the increased reactivity of 2˚ sites located more distal to EWGs. This conclusion is further evidenced by the increased reaction times necessary for strongly deactivated substrates under the DCAA conditions (**2j**). Nitrile and malononitrile groups are among the most deactivating, as the corresponding substrates were oxidized selectively at 2˚ C–H sites five to six carbons removed from the α-carbon(**2k-2m**). Multiple Lewis basic EWGs performed synergistically to deactivate proximal 2˚ sites (**2n**). Carbocyclic substrates tended to give lower site-selectivity relative to linear analogs, even when more deactivating conditions are employed. (**2o-2q**).

Table 2: Scope of Ru Catalyzed 2˚ C–H Bond Oxidation.[a]

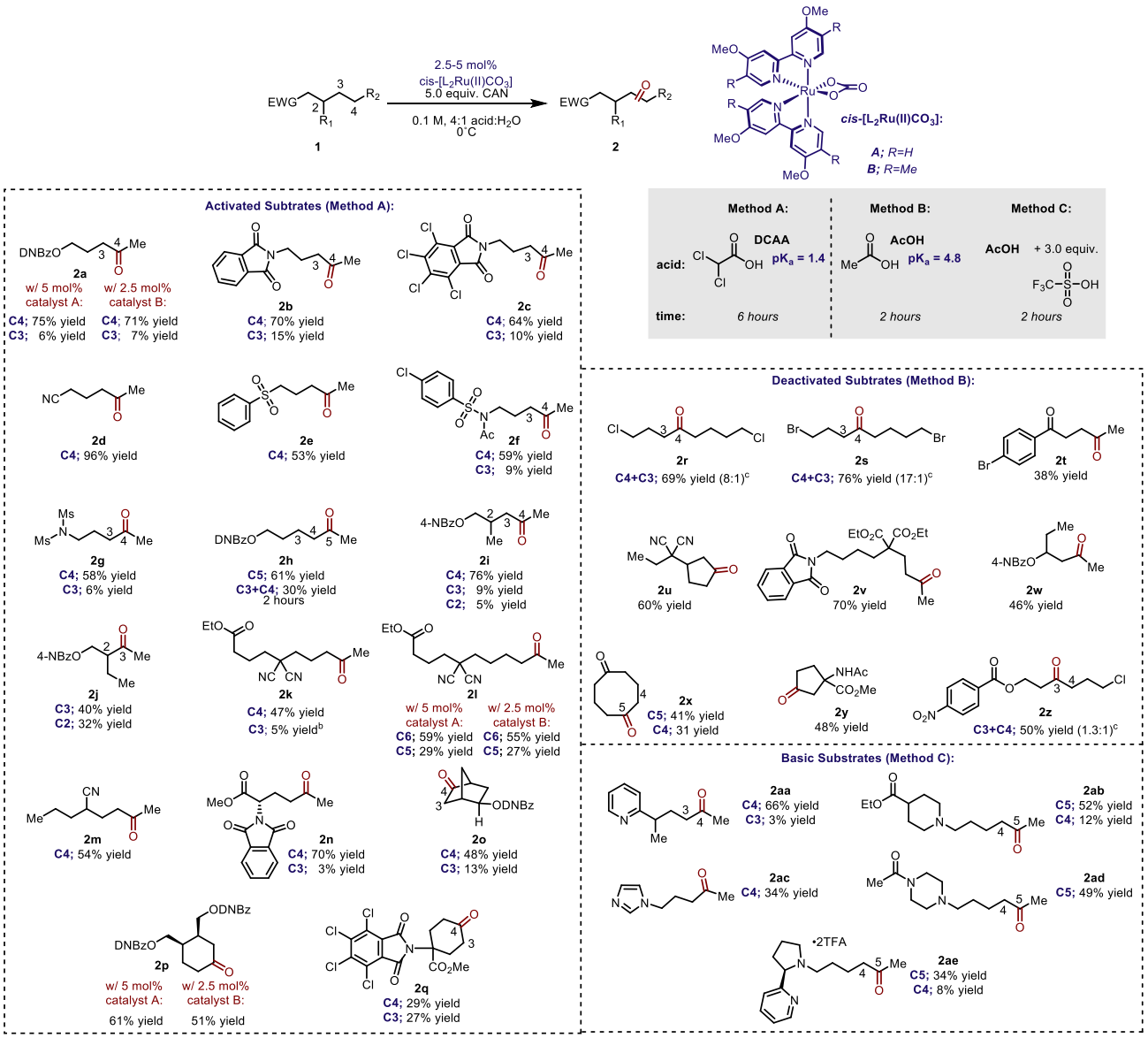

[a] 1.0 mmol scale with 5 mol% of catalyst **A** unless otherwise noted. Yields refer to isolated yield of each isomer, and are thus not a true representation of the site-selectivity produced by the reaction. [b]Yield determined by ^{1}H NMR integration against hexamethyldisiloxane (HMDSO)internal standard. [c] Ratio of major and minor isomers.

Throughout the course of our studies, we recognized that not all reactions benefit from using DCAA as co-solvent. Generally, for reactions with strongly deactivated substrates, which tend to give a single oxidation product, the use of DCAA was not necessary. In addition, substrates that lack sufficiently Lewis basic functional groups show little improvement under DCAA conditions (**2r** and **2s**). In these cases, the use of AcOH/H_2O as solvent was found to give similar or better yields to the DCAA

conditions. Finally, as previously demonstrated by our labs and others,[33,34] oxidatively labile amines can be protected through in situ protonation while simultaneously deactivating nearby C–H bonds. In these cases, a strong acid such as triflic acid (TfOH) was used to prevent unwanted amine oxidation products (**2aa-2ae**).

After evaluating a wider array of substrates (including ester substrates from **Figure 3** and substrates in **Table 2**), the correlation of the data with our multivariate model, $(E_{\sigma C–Hdist} - E_{\sigma\ C–Hprox})^{Boltz}$ is less clear (**Figure 4**). We hypothesized that H–bonding interactions between substrate and solvent underlie the disparate influence of both functional group and solvent acidity on site selectivity, and thus reasoned that it would be important to describe this feature in our model. For example, halogenated substrates **2r** and **2s** (**Table 2**) have comparatively weak H–bond acceptor capability relative to more Lewis basic substrates such as esters or nitriles. Ultimately, we found that model functional groups could be used to simulate H–bonding interactions between the substrate and the respective acid solvent at the M06-2X/def2-TZVP level of theory with the SMD solvation model for acetic acid.[46] Additionally, incorporating a parameter that describes the number of bonds between the EWG and the minor oxidation site provided a better fit for our model ($Location_{Minor}$); this parameter describes the reduction in the ability of the EWG and H–bonding interactions to deactivate C–H bonds that are located multiple bonds away. Altogether a three-parameter model was obtained ($R^2 = 0.85$), which demonstrates that $(E_{\sigma C–Hdist} - E_{\sigma\ C–Hprox})^{Boltz}$ as the most important component for determining selectivity. Interestingly, we found that the selectivity of amine substrates is not well described by this model, presumably due to the fact that amines undergo complete protonation under the reaction conditions rather than engaging in H–bonding interactions.

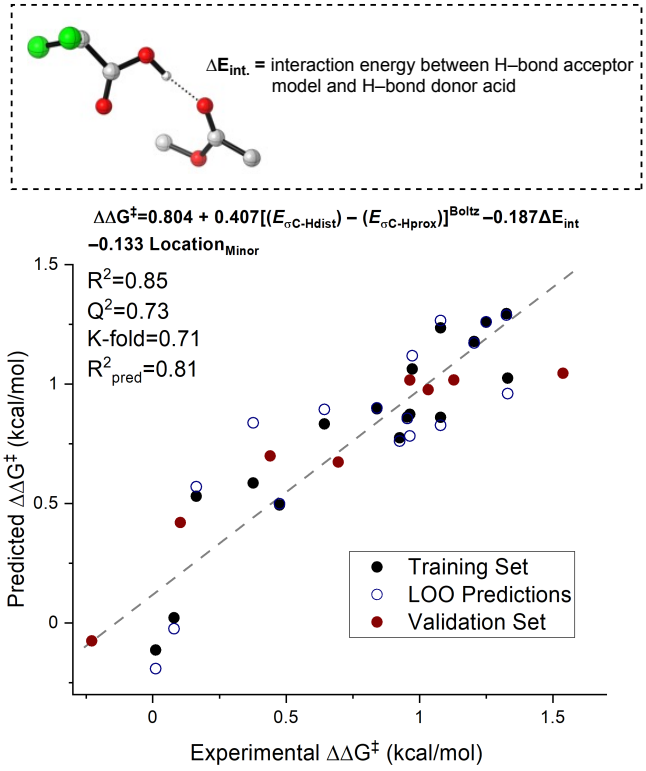

Figure 4: MLR model relating substrates parameters with the observed site-selectivity of oxidation. Selectivity was obtained via analysis of crude ^{1}H NMR spectra prior to isolation.

In summary, we have developed an operationally simple protocol for the direct oxidation of 2˚ C–H bonds catalyzed by a Ru-catalyst. We have demonstrated that judicious selection of protecting group for alcohols enhances product selectivity. A strongly acidic reaction medium, which results in strong H-bonding between substrate and solvent, further boosts site-selectivity. Evaluating the properties of the substrate (H-bonding capability, number of potential oxidation sites, etc.) is necessary prior to selecting reaction/solvent conditions. A statistical model to gain insight into factors controlling product distributions highlights that differences in C–H bond energies ($E_{\sigma C–H}$) serve as a useful predictor of site selectivity. Finally, we have demonstrated that relatively minor changes to ligand structure can provide more efficient catalysis.

ASSOCIATED CONTENT

The Supporting Information is available free of charge at

Experimental procedures for all reactions; spectroscopic characterization data for all new compounds; detailed computational methods; copies of ^{1}H and ^{13}C NMR spectra; and cartesian coordinates (PDF)

AUTHOR INFORMATION

Corresponding Author

J. Du Bois–Department of Chemistry, Stanford University, Stanford, California 94305, United States;orcid.org/0000-0001-7847-1548; Email:jdubois@stanford.edu

Matthew S. Sigman–Department of Chemistry, University of Utah, Salt Lake City, Utah 84112, United States; orcid.org/0000-0002-5746-8830; Email:sigman@chem.utah.edu

Authors

Jeremy D. Griffin–Department of Chemistry, University of Utah, Salt Lake City, Utah 84112, United States

David B. Vogt–Department of Chemistry, University of Utah, Salt Lake City, Utah 84112, United States

Notes: The authors declare no competing financial interest.

Supporting Information:

The Supporting Information is available free of charge at Experimental procedures for all reactions, spectroscopic characterization data for all new compounds, detailed computational methods, copies of 1H and 13C NMR spectra, and Cartesian coordinates (PDF)

ACKNOWLEDGEMENTS

We thank the National Science Foundation under the Center for Chemical Innovation in Selective C–H Functionalization (CHE-1700982) for financial support of this work. J.D.G. thanks the

National Institute of Health for financial support through a F32 Ruth L. Kirschtein NRSA fellowship (F32 GM129980). Computational resources were provided from the Center for High Performance Computing (CHPC) at the University of Utah. NMR results included in this report were recorded at the David M. Grant NMR Center, a University of Utah Core Facility. Funds for construction of the Center and the helium recovery system were obtained from the University of Utah and the National Institutes of Health awards 1C06RR017539-01A1 and3R01GM063540-17W1, respectively. NMR instruments were purchased with support of the University of Utah and the National Institutes of Health award 1S10OD25241-01.

REFERENCES

(1) Mello, R.; Fiorentino, M.; Sciacovelli, O.; Curci, R. On the Isolation and Characterization of Methyl (Trifluoromethyl) Dioxirane. *J. Org. Chem.* **1988**, *53* (16), 3890–3891. https://doi.org/10.1021/jo00251a053.

(2) Bovicelli, P.; Lupattelli, P.; Mincione, E.; Prencipe, T.; Curci, R. Oxidation of Natural Targets by Dioxiranes. 2. Direct Hydroxylation at the Side Chain C-25 of Cholestane Derivatives and of Vitamin D3 Windaus-Grundmann Ketone. *J. Org. Chem.* **1992**, *57* (19), 5052–5054. https://doi.org/10.1021/jo00045a004.

(3) DesMarteau, D. D.; Donadelli, A.; Montanari, V.; Petrov, V. A.; Resnati, G. Mild and Selective Oxyfunctionalization of Hydrocarbons by Perfluorodialkyloxaziridines. *J. Am. Chem. Soc.* **1993**, *115* (11), 4897–4898. https://doi.org/10.1021/ja00064a063.

(4) Curci, R.; Dinoi, A.; Rubino, M. F. Dioxirane Oxidations: Taming the Reactivity-Selectivity Principle. *Pure Appl. Chem.* **1995**, *67* (5), 811–822. https://doi.org/10.1351/pac199567050811.

(5) D'Accolti, L.; Dinoi, A.; Fusco, C.; Russo, A.; Curci, R. Oxyfunctionalization of Non-Natural Targets by Dioxiranes. 5. Selective Oxidation of Hydrocarbons Bearing Cyclopropyl Moieties1. *J. Org. Chem.* **2003**, *68* (20), 7806–7810. https://doi.org/10.1021/jo034768o.

(6) Curci, R.; D'Accolti, L.; Fusco, C. A Novel Approach to the Efficient Oxygenation of Hydrocarbons under Mild Conditions. Superior Oxo Transfer Selectivity Using Dioxiranes. *Acc. Chem. Res.* **2006**, *39* (1), 1–9. https://doi.org/10.1021/ar050163y.

(7) Litvinas, N. D.; Brodsky, B. H.; Du Bois, J. C H Hydroxylation Using a Heterocyclic Catalyst and Aqueous H2O2. *Angew. Chem. Int. Ed.* **2009**, *48* (25), 4513–4516. https://doi.org/10.1002/anie.200901353.

(8) Chen, K.; Eschenmoser, A.; Baran, P. S. Strain Release in C H Bond Activation? *Angew. Chem. Int. Ed.* **2009**, *48* (51), 9705–9708. https://doi.org/10.1002/anie.200904474.

(9) Newhouse, T.; Baran, P. S. If C H Bonds Could Talk: Selective C H Bond Oxidation. *Angew. Chem. Int. Ed.* **2011**, *50* (15), 3362–3374. https://doi.org/10.1002/anie.201006368.

(10) Nicolaou, K. C.; Montagnon, T.; Baran, P. S.; Zhong, Y.-L. Iodine(V) Reagents in Organic Synthesis. Part 4. o-Iodoxybenzoic Acid as a Chemospecific Tool for Single Electron Transfer-Based Oxidation Processes. *J. Am. Chem. Soc.* **2002**, *124* (10), 2245–2258. https://doi.org/10.1021/ja012127+.

(11) Ali Shaikh, T. M.; Emmanuvel, L.; Sudalai, A. NaIO4-Mediated Selective Oxidation of Alkylarenes and Benzylic Bromides/Alcohols to Carbonyl Derivatives Using Water as Solvent. *J. Org. Chem.* **2006**, *71* (13), 5043–5046. https://doi.org/10.1021/jo0606305.

(12) Dohi, T.; Takenaga, N.; Goto, A.; Fujioka, H.; Kita, Y. Clean and Efficient Benzylic C−H Oxidation in Water Using a Hypervalent Iodine Reagent: Activation of Polymeric Iodosobenzene with KBr in the Presence of Montmorillonite-K10. *J. Org. Chem.* **2008**, *73* (18), 7365–7368. https://doi.org/10.1021/jo8012435.

(13) Zhao, Y.; Yim, W.-L.; Tan, C. K.; Yeung, Y.-Y. An Unexpected Oxidation of Unactivated Methylene C–H Using DIB/TBHP Protocol. *Org. Lett.* **2011**, *13* (16), 4308–4311. https://doi.org/10.1021/ol2016466.

(14) Jiang, J.; Ramozzi, R.; Moteki, S.; Usui, A.; Maruoka, K.; Morokuma, K. Mechanism of Metal-Free C–H Activation of Branched Aldehydes and Acylation of Alkenes Using Hypervalent Iodine Compound: A Theoretical Study. *J. Org. Chem.* **2015**, *80* (18), 9264–9271. https://doi.org/10.1021/acs.joc.5b01695.

(15) Yamazaki, S. Chromium(VI) Oxide-Catalyzed Benzylic Oxidation with Periodic Acid. *Org. Lett.* **1999**, *1* (13), 2129–2132. https://doi.org/10.1021/ol991175k.

(16) Lee, S.; Fuchs, P. L. Chemospecific Chromium[VI] Catalyzed Oxidation of C−H Bonds at −40 °C. *J. Am. Chem. Soc.* **2002**, *124* (47), 13978–13979. https://doi.org/10.1021/ja026734o.

(17) Gómez, L.; Garcia-Bosch, I.; Company, A.; Benet-Buchholz, J.; Polo, A.; Sala, X.; Ribas, X.; Costas, M. Stereospecific C H Oxidation with H2O2 Catalyzed by a Chemically Robust Site-Isolated Iron Catalyst. *Angew. Chem.* **2009**, *121* (31), 5830–5833. https://doi.org/10.1002/ange.200901865.

(18) Chen, M. S.; White, M. C. Combined Effects on Selectivity in Fe-Catalyzed Methylene Oxidation. *Science* **2010**, *327* (5965), 566–571. https://doi.org/10.1126/science.1183602.

(19) Bigi, M. A.; Liu, P.; Zou, L.; Houk, K. N.; White, M. C. Cafestol to Tricalysiolide B and Oxidized Analogues: Biosynthetic and Derivatization Studies Using Non-Heme Iron Catalyst Fe(PDP). *Synlett* **2012**, *23* (19), 2768–2772. https://doi.org/10.1055/s-0032-1317708.

(20) Bigi, M. A.; Reed, S. A.; White, M. C. Directed Metal (Oxo) Aliphatic C–H Hydroxylations: Overriding Substrate Bias. *J. Am. Chem. Soc.* **2012**, *134* (23), 9721–9726. https://doi.org/10.1021/ja301685r.

(21) Gómez, L.; Canta, M.; Font, D.; Prat, I.; Ribas, X.; Costas, M. Regioselective Oxidation of Nonactivated Alkyl C–H Groups Using Highly Structured Non-Heme Iron Catalysts. *J. Org. Chem.* **2013**, *78* (4), 1421–1433. https://doi.org/10.1021/jo302196q.

(22) Gormisky, P. E.; White, M. C. Catalyst-Controlled Aliphatic C–H Oxidations with a Predictive Model for Site-Selectivity. *J. Am. Chem. Soc.* **2013**, *135* (38), 14052–14055. https://doi.org/10.1021/ja407388y.

(23) Howell, J. M.; Feng, K.; Clark, J. R.; Trzepkowski, L. J.; White, M. C. Remote Oxidation of Aliphatic C–H Bonds in Nitrogen-Containing Molecules. *J. Am. Chem. Soc.* **2015**, *137* (46), 14590–14593. https://doi.org/10.1021/jacs.5b10299.

(24) Nanjo, T.; de Lucca, E. C.; White, M. C. Remote, Late-Stage Oxidation of Aliphatic C–H Bonds in Amide-Containing Molecules. *J. Am. Chem. Soc.* **2017**, *139* (41), 14586–14591. https://doi.org/10.1021/jacs.7b07665.

(25) Milan, M.; Bietti, M.; Costas, M. Enantioselective Aliphatic C–H Bond Oxidation Catalyzed by Bioinspired Complexes. *Chem. Commun.* **2018**, *54* (69), 9559–9570. https://doi.org/10.1039/C8CC03165G.

(26) Adams, A. M.; Du Bois, J.; Malik, H. A. Comparative Study of the Limitations and Challenges in Atom-Transfer C–H Oxidations. *Org. Lett.* **2015**, *17* (24), 6066–6069. https://doi.org/10.1021/acs.orglett.5b03047.

(27) Dantignana, V.; Milan, M.; Cussó, O.; Company, A.; Bietti, M.; Costas, M. Chemoselective Aliphatic C–H Bond Oxidation Enabled by Polarity Reversal. *ACS Cent. Sci.* **2017**, *3* (12), 1350–1358. https://doi.org/10.1021/acscentsci.7b00532.

(28) Milan, M.; Bietti, M.; Costas, M. Highly Enantioselective Oxidation of Nonactivated Aliphatic C–H Bonds with Hydrogen Peroxide Catalyzed by Manganese Complexes. *ACS Cent. Sci.* **2017**, *3* (3), 196–204. https://doi.org/10.1021/acscentsci.6b00368.

(29) Zhao, J.; Nanjo, T.; de Lucca, E. C.; White, M. C. Chemoselective Methylene Oxidation in Aromatic Molecules. *Nat. Chem.* **2019**, *11* (3), 213–221. https://doi.org/10.1038/s41557-018-0175-8.

(30) Chambers, R. K.; Zhao, J.; Delaney, C. P.; White, M. C. Chemoselective Tertiary C−H Hydroxylation for Late-Stage Functionalization with Mn(PDP)/Chloroacetic Acid Catalysis. *Adv. Synth. Catal.* **2020**, *362* (2), 417–423. https://doi.org/10.1002/adsc.201901472.

(31) Horn, E. J.; Rosen, B. R.; Chen, Y.; Tang, J.; Chen, K.; Eastgate, M. D.; Baran, P. S. Scalable and Sustainable Electrochemical Allylic C–H Oxidation. *Nature* **2016**, *533* (7601), 77–81. https://doi.org/10.1038/nature17431.

(32) Kawamata, Y.; Yan, M.; Liu, Z.; Bao, D.-H.; Chen, J.; Starr, J. T.; Baran, P. S. Scalable, Electrochemical Oxidation of Unactivated C–H Bonds. *J. Am. Chem. Soc.* **2017**, *139* (22), 7448–7451. https://doi.org/10.1021/jacs.7b03539.

(33) Mack, J. B. C.; Gipson, J. D.; Du Bois, J.; Sigman, M. S. Ruthenium-Catalyzed C–H Hydroxylation in Aqueous Acid Enables Selective Functionalization of Amine Derivatives. *J. Am. Chem. Soc.* **2017**, *139* (28), 9503–9506. https://doi.org/10.1021/jacs.7b05469.

(34) Robinson, S. G.; Mack, J. B. C.; Alektiar, S. N.; Du Bois, J.; Sigman, M. S. Electrochemical Ruthenium-Catalyzed C–H Hydroxylation of Amine Derivatives in Aqueous Acid. *Org. Lett.* **2020**, *22* (18), 7060–7063. https://doi.org/10.1021/acs.orglett.0c01313.

(35) Dobson, J. C.; Meyer, T. J. Redox Properties and Ligand Loss Chemistry in Aqua/Hydroxo/Oxo Complexes Derived from Cis- and Trans-[(Bpy)2RuII(OH2)2]2+. *Inorg. Chem.* **1988**, *27* (19), 3283–3291. https://doi.org/10.1021/ic00292a008.

(36) Mack, J. B. C.; Walker, K. L.; Robinson, S. G.; Zare, R. N.; Sigman, M. S.; Waymouth, R. M.; Du Bois, J. Mechanistic Study of Ruthenium-Catalyzed C–H Hydroxylation Reveals an Unexpected Pathway for Catalyst Arrest. *J. Am. Chem. Soc.* **2019**, *141* (2), 972–980. https://doi.org/10.1021/jacs.8b10950.

(37) *CRC Handbook of Chemistry and Physics*, 90th ed.; University of Rhode Island.

(38) Hilton, M. C.; Dolewski, R. D.; McNally, A. Selective Functionalization of Pyridines via Heterocyclic Phosphonium Salts. *J. Am. Chem. Soc.* **2016**, *138* (42), 13806–13809. https://doi.org/10.1021/jacs.6b08662.

(39) Dolewski, R. D.; Hilton, M. C.; McNally, A. 4-Selective Pyridine Functionalization Reactions via Heterocyclic Phosphonium Salts. *Synlett* **2018**, *29* (1), 8–14. https://doi.org/10.1055/s-0036-1591850.

(40) Santiago, C. B.; Milo, A.; Sigman, M. S. Developing a Modern Approach To Account for Steric Effects in Hammett-Type Correlations. *J. Am. Chem. Soc.* **2016**, *138* (40), 13424–13430. https://doi.org/10.1021/jacs.6b08799.

(41) Santiago, C. B.; Guo, J.-Y.; Sigman, M. S. Predictive and Mechanistic Multivariate Linear Regression Models for Reaction Development. *Chem. Sci.* **2018**, *9* (9), 2398–2412. https://doi.org/10.1039/C7SC04679K.

(42) Harder, E.; Damm, W.; Maple, J.; Wu, C.; Reboul, M.; Xiang, J. Y.; Wang, L.; Lupyan, D.; Dahlgren, M. K.; Knight, J. L.; Kaus, J. W.; Cerutti, D. S.; Krilov, G.; Jorgensen, W. L.; Abel, R.; Friesner, R. A. OPLS3: A Force Field Providing Broad Coverage of Drug-like Small Molecules and Proteins. *J. Chem. Theory Comput.* **2016**, *12* (1), 281–296. https://doi.org/10.1021/acs.jctc.5b00864.

(43) Roos, K.; Wu, C.; Damm, W.; Reboul, M.; Stevenson, J. M.; Lu, C.; Dahlgren, M. K.; Mondal, S.; Chen, W.; Wang, L.; Abel, R.; Friesner, R. A.; Harder, E. D. OPLS3e: Extending Force Field Coverage for Drug-Like Small Molecules. *J. Chem. Theory Comput.* **2019**, *15* (3), 1863–1874. https://doi.org/10.1021/acs.jctc.8b01026.

(44) Zhao, Y.; Truhlar, D. G. The M06 Suite of Density Functionals for Main Group Thermochemistry, Thermochemical Kinetics, Noncovalent Interactions, Excited States, and Transition Elements: Two New Functionals and Systematic Testing of Four M06-Class Functionals and 12 Other Functionals. *Theor. Chem. Acc.* **2008**, *120* (1), 215–241. https://doi.org/10.1007/s00214-007-0310-x.

(45) Weigend, F.; Ahlrichs, R. Balanced Basis Sets of Split Valence, Triple Zeta Valence and Quadruple Zeta Valence Quality for H to Rn: Design and Assessment of Accuracy. *Phys. Chem. Chem. Phys.* **2005**, *7* (18), 3297–3305. https://doi.org/10.1039/B508541A.

(46) Marenich, A. V.; Cramer, C. J.; Truhlar, D. G. Universal Solvation Model Based on Solute Electron Density and on a Continuum Model of the Solvent Defined by the Bulk Dielectric Constant and Atomic Surface Tensions. *J. Phys. Chem. B* **2009**, *113* (18), 6378–6396. https://doi.org/10.1021/jp810292n.